

Continuous Scanning Measurement of Surface Compliance Distribution from Remote Position Using Rotated Mirror

Masahiro Fujiwara and Hiroyuki Shinoda

Department of Information Physics and Computing, University of Tokyo, Tokyo, Japan
(Tel : +81-3-5841-6927; E-mail: masahiro_fujiwara@ipc.i.u-tokyo.ac.jp, hiroyuki_shinoda@k.u-tokyo.ac.jp)

Abstract: In this paper, we propose a continuous scanning measurement method of surface compliance distribution from remote position. This method measures the surface displacement distribution generated by ultrasound acoustic radiation pressure using a rotated mirror driven by a stepping motor. The two dimensional scanning of the displacement measurement on the surface can be continuously performed by a motorized mechanical stage moving in a direction parallel to the mirror rotation axis. This paper also evaluates the theoretical limit of the scanning speed which depends on the pressurization process and the viscosity of the measured object.

Keywords: Compliance distribution, Remote measurement, Tactile sensing, Hardness evaluation.

1. INTRODUCTION

Simultaneous sharing of tactile sensation among many people is a challenging theme in haptic transmission. For simultaneous haptic sharing, it is necessary to generate the numerical object model [1] which includes its haptic information such as shape, hardness, tactile texture, temperature, etc. Furthermore, high-speed haptic information sensing is desired for synchronized display of visual, audio, and haptic information. For high-speed spatial distribution sensing of haptic information, a remote measurement system is required.

We have proposed a remote measurement method of surface compliance distribution as one of the haptic information which is perceptible by hand exploration [1]. The compliance is a critical property for recognition of an object and simply quantified as spring constant on a point in the surface. The proposed method utilizes acoustic radiation pressure of convergent ultrasound beam for pressing a point in an object surface. The generated displacement on the point is measured by a triangulation-type laser displacement sensor. The scanning of the pressurization point and displacement measuring point are performed by an ultrasound phased array and a motorized XY-axis mechanical stage to which the laser displacement sensor is attached, respectively. The scanning time of the measurement point for obtaining the compliance distribution is limited by the movement time of the laser displacement sensor.

In this paper, we propose a scanning method using a continuously rotated mirror to fold the optical axis of the laser displacement sensor for shortening of the measurement time. This method does not require movement of the sensor head which has large mass in a single direction. The scanning of the remaining direction is performed by a motorized mechanical stage as before. The theoretical limit of measurement speed is also surveyed for synchronous continuous scanning of the pressurization and displacement measuring point.

2. NONCONTACT COMPLIANCE MEASUREMENT USING ACOUSTIC

RADIATION PRESSURE

The measured hardness is defined in this paper as the ratio of vertical force F applied to a spot circle area on an object surface to vertical displacement Δh at its center. And the corresponding compliance is the reciprocal of the hardness. Linear deformation is assumed in this model so that the compliance c is equal to a unique value $\Delta h / F$ at each point. In our measurement, the vertical force F is sufficiently small to satisfy this assumption. The hardness and the compliance defined like this depend on the pressurization area and its shape. Supposing a virtual situation that a human finger pushes the surface, we choose about 1cm diameter circle pushed area as our previous work [1].

Our method is a direct measurement method which presses the target surface and measures the displacement caused by the pressurization. Our implemented system is composed of an airborne ultrasound phased array, which is the identical to a tactile display developed in [2], and a laser displacement sensor (LK-G80, Keyence corp., Japan) based on triangulation principle. The ultrasound phased array generates convergent ultrasound beam which pushes a target point on the surface by acoustic radiation pressure illustrated in following section. The laser displacement sensor measures height from a reference plane determined by the arrangement of the sensor. The hardness distribution is obtained by scanning the measuring points: the pressing point and the displacement sensing point. In previous work, the laser displacement sensor is moved by an auto XY-axis mechanical stage (SGSP (CS) 26-200(X), SIGMA KOKI CO., LTD., Japan) and thus the measuring time is limited by the stage moving time.

2.1 Acoustic radiation pressure

Ultrasound acoustic radiation pressure, which is used to press the target surface, is constant pressure derived from non-linearity of medium [3]. This phenomenon appears remarkably in high amplitude sound by increasing the second order term of wave equation. For propagation of large amplitude ultrasound, the acoustic radiation pressure appears as the DC component of

sound pressure. Assuming vertical incident on an object surface, the acoustic radiation pressure P is represented by

$$P = (1 + R)E = (1 + R) \frac{p_0^2}{\rho c^2} \quad (1)$$

where R is the reflection coefficient between the object and the medium, E , ρ , c , p_0 are acoustic energy density, the medium density, the sound speed, and the RMS sound pressure of ultrasound, respectively. Since R is nearly equal to 1 if the ultrasound incidents to solid or liquid surface from air as our supposing situation, Eq. (1) is shortened to

$$P \approx 2E = \frac{2p_0^2}{\rho c^2}. \quad (2)$$

For oblique incidence, the magnitude of the acoustic radiation pressure is described in [4]. The incident component F_i of the acoustic radiation force on an area S is $F_i = ES \cos\theta$, where θ is the incident angle as shown in Fig. 1. Thus total acoustic radiation force is $F = (F_i + F_r)\cos\theta$, where F_r is the reflective component of the acoustic radiation force. Since $F_i = F_r$ in case of the perfectly reflective surface like our situation, the total acoustic radiation pressure is represented as

$$P = \frac{F}{S} = 2E \cos^2 \theta. \quad (3)$$

The acoustic radiation force occurs in the normal direction of the reflected surface.

A concrete value of the acoustic radiation pressure for a typical ultrasound transducer of 117dB_{SPL} sound pressure (T4010A1, NIPPON CERAMIC CO., LTD, Japan.) is approximately 1.41mPa in standard air (0 °C, 1 atm). For obtaining sufficient large displacement of human skin like hardness object, larger sound pressure is necessary. And the pressure point position should be updated at high-speed. These requirements is satisfied by using an ultrasound phased array illustrated in the following section.

2.2 Spot pressurization by ultrasound phased array

We utilize an airborne ultrasound phased array to generate convergent ultrasound beam. The ultrasound phased array have phase controlled ultrasound transducers arranged as a grid pattern on a plane. The phased array generates a focal by controlling driving phase of each ultrasound transducer so that each phase agrees at one point in space. The amplitude of sound pressure around the focal in a plane parallel to the square-shaped phased array is approximated as

$$p(x, y) \approx \sqrt{2} p_r N^2 \left| \text{sinc} \left(\frac{\pi N d (x - x_c)}{\lambda r}, \frac{\pi N d (y - y_c)}{\lambda r} \right) \right| \quad (4)$$

where (x_c, y_c, r) is the coordinate of the focal point, p_r is the RMS sound pressure from each transducer at the propagation distance r , N is the number of transducers in the one side, d and λ are the diameter of the transducer and the wavelength of the ultrasound, respectively. The two-variable sinc function is defined as $\text{sinc}(x, y) := \sin(x)\sin(y)/(xy)$ in case of $xy \neq 0$, $\text{sinc}(x, y) := 1$ in case of $xy = 0$. For derivation of Eq. (4),

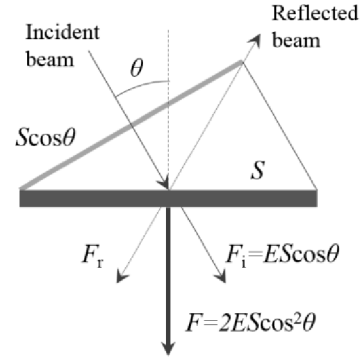


Fig. 1 The acoustic radiation force for oblique incident ultrasound.

Fresnel approximation has been applied and it is assumed that a number N is sufficiently large. The RMS value of the sound pressure on the focal point is calculated as $p(x_c, y_c) = p_r N^2$, which is the summation of the sound pressure from N^2 transducers. The acoustic radiation pressure at the focal is determined by substituting the sound pressure for Eq. (2) for vertical incident:

$$P = \frac{2p_r^2}{\rho c^2} N^4. \quad (5)$$

When the focal point is shifted from the center axis of the array, the wave-front at the focal becomes unparallel to the array because of contribution unbalance of each transducer for forming the focal. For oblique incident, the acoustic radiation pressure is corrected by Eq. (3) as shown in [4].

The diameter of the focal is regarded as the full width at half maximum (FWHM) of the acoustic radiation pressure distribution. The FWHM of the squared sinc function is nearly equal to 2.78, thus the diameter of the focal $D_0 = 2.78 \lambda r / (\pi N d)$. In case of the focal length r is nearly equal to the array aperture size Nd , which satisfies Fresnel approximation and minimizes the diameter, $D_0 = 0.88 \lambda$. Since the diameter D_0 is independent to the focal length r in this condition, it enables to press a spot area on a surface from a remote position by using a large aperture array.

The updating time limitation of the focal position depends on the sound speed c and the aperture size Nd because the updated phase distribution on the array reaches the new focal point in different delays from each transducer.

3. DISPLACEMENT MEASUREMENT BY ROTATED MIRROR

The displacement measuring point on a target object is scanned by a continuously rotated mirror for x -axis scanning and by a motorized mechanical stage for y -axis scanning as shown in Fig. 2. The rotated mirror is controlled by a stepping motor (CSA-UA60D1, Shinano Kenshi Co., LTD, Japan). The two-dimensional scanning on an object surface is performed by driving these mechanisms simultaneously.

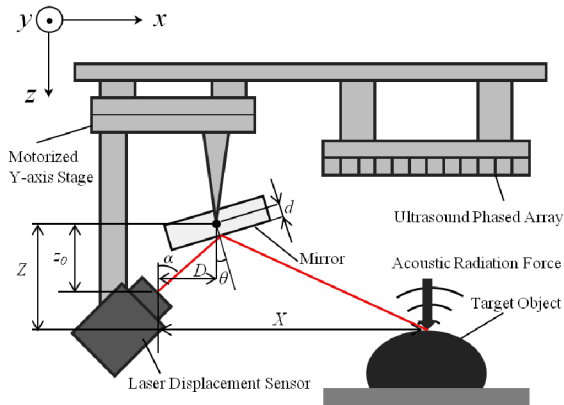


Fig. 2 Arrangement of the surface compliance distribution measurement system using a rotated mirror scanning.

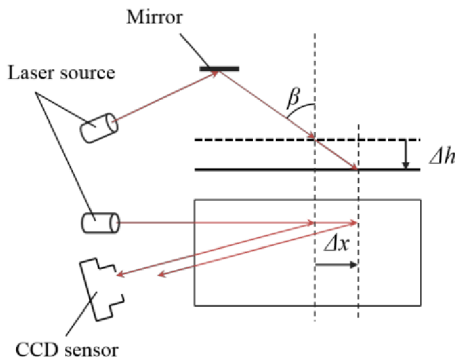


Fig. 3 Deviation of the laser spot of a displacement sensor by the surface displacement.

In Fig. 2, the ultrasound phased array and the motorized Y-axis stage are mounted on the same base. The conventional motorized XY-axis mechanical stage have required starting and stopping of the movement periodically for two-dimensional scanning. In contrast, by using the rotated mirror, those movements time are not required. The laser displacement sensor is attached to a manual Z-axis mechanical stage. The rotated mirror is attached so that the rotation axis is perpendicular to the laser and is parallel to the triangulation plane. This arrangement has an advantage that it is easy to correct the measured data to the displacement on the object surface from the mirror angle.

In Fig. 3, it is illustrated that the laser spot at incident angle $\beta (= \alpha + 2\theta)$ displaces Δx on the surface when the target surface is Δh dented. Because $\Delta x = \Delta h \tan\beta$, the measured displacement Δh_d by the sensor is represented as

$$\Delta h_d = \sqrt{(\Delta x)^2 + (\Delta h)^2} = \Delta h \sqrt{(\tan \beta)^2 + 1}. \quad (6)$$

The measured displacement Δh_d can be corrected by Eq. (6) and the current mirror angle θ .

The displacement sensor has to measure two times at the same point before and after deformation for displacement sensing, since the sensor measures only height from a reference plane. For a pressing period, the

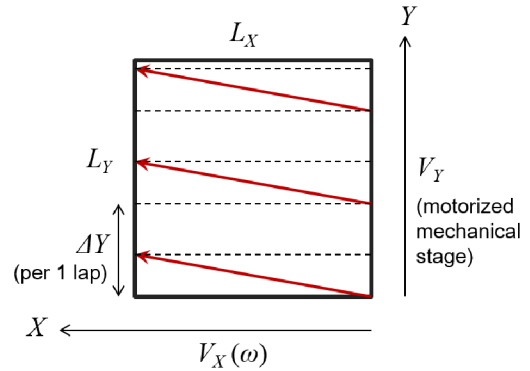


Fig. 4 Scanning line of the displacement measurement laser on the measured area.

theoretical limitation of the displacement measurement time depends on deformation time of the object. The upper limit of the scanning velocity is

$$v_{\max} = w / \tau \quad (7)$$

where w is the pressurization width and τ is the time constant of the displacement transition. The width w is comparable to the diameter of the focal D_0 .

In Fig.4, the proceeding distance ΔY while the mirror rotates once is

$$\Delta Y = 2\pi V_Y / \omega \quad (8)$$

where V_Y is Y-axis moving velocity of the scanning point and ω is the angular velocity of the rotated mirror. Under the condition that the upper limit of scanning speed is v_{\max} , an inequality

$$v_{\max} > \sqrt{V_X^2 + V_Y^2} \approx V_X \quad (9)$$

holds where V_X is X-axis moving velocity of the scanning point and V_Y is that of the motorized mechanical stage.

4. EXPERIMENTAL RESULTS AND DISCUSSION

For verifying the scanning method by the rotated mirror, we measured displacement response on liquid surface for pressurization. In this experiment, reproducibility of surface compliance measurement for the different measuring point is confirmed.

An appearance of the experimental setup is shown in Fig.5. The dimension values in Fig. 2 are $z_0 = 155\text{mm}$, $D = 23.5\text{mm}$, $d = 5.0\text{mm}$, $\alpha = 9.6^\circ$. The stepping motor is 0.1125° step angle and was input 43.5Hz pulse wave. The motorized mechanical stage was fixed in this experiment. In this setup, the scanning speed on the surface is 78.6mm/s .

The aperture size Nd of the ultrasound phased array is equal to 18cm and the transducer frequency is 40kHz . Thus the measurable range is about 18cm distant from the array, and the diameter of the focal is about 7.5mm in standard air. For 40kHz frequency ultrasound, whose attenuation rate is 1dB/m [5], the absorption attenuation in air is less than 5% at 18cm distant. The acoustic

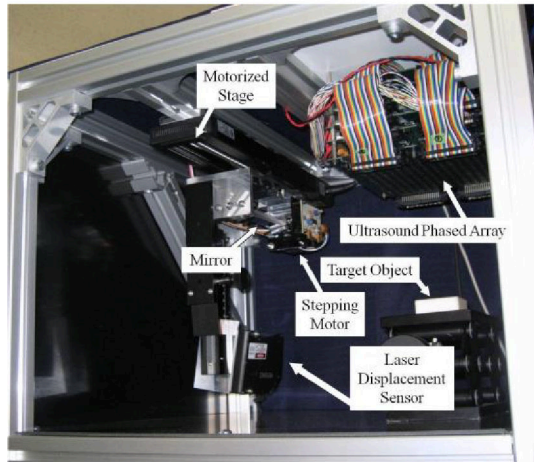


Fig. 5 Appearance of the surface compliance distribution measurement system using a rotated mirror scanning.

radiation force on the focal point is about 17mN. The minimum update time of the focal position is 0.25ms which is comparable to the difference between the propagation time from the center transducer and it from the edge transducer.

The target surface is composed of solid acrylic surface and water surface as shown in Fig. 6(a). The accurate prediction of the displacement response on the water surface pressed by acoustic radiation pressure is generally difficult due to complexity of fluid behavior. Although there is this difficulty, large displacement is expected since the shear force of water is lower than that of an elastic body.

The measured displacement distribution is shown in Fig. 6(b). The average displacement on the water area ($0 < t < 0.7\text{sec}$, $0.7\text{sec} < t < 1.25\text{sec}$) is remarkably larger than that on the solid acrylic area ($0.7\text{sec} < t < 1.25\text{sec}$). However, the variance of the displacement on the water area is also large ($\sim 1\text{mm}$), especially in the right area ($0.7\text{sec} < t < 1.25\text{sec}$) where the laser incident angle β is large.

Two factors are considered as the cause of the large variance. First, the disturbance of the water surface by the pressurization causes unstable displacement distribution. That perturbation may affect the increase of the variance according to Eq. (6). Second, the vibration produced by the periodical structure of the stepping motor causes unexpected rotation of mirror. The rotation angle θ for correction of displacement using Eq. (6) deviates periodically from the set angle by input pulses. To solve these problems, the actuator should be replaced with a vibrationless one. In addition to it, coaxial setting of the pressurization and displacement measurement for reducing the incident angle β is desired.

4. CONCLUSION AND FUTURE WORK

In this research, we proposed a scanning method of a remote surface compliance distribution measurement by using a rotated mirror. The measured displacement has large variance for compliance measurement. For

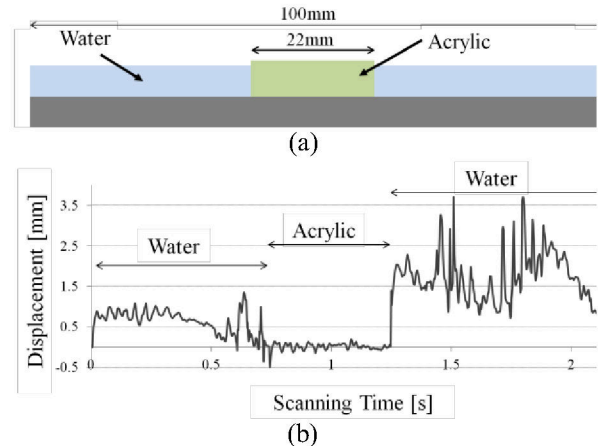


Fig. 6 (a) Cross section of measured surface. (b) Measured displacement distribution scanned by the rotated mirror.

improvement of measurement accuracy, an actuator with less vibration and coaxial setting of pressurization and displacement measurement is required.

ACKNOWLEDGEMENTS

This work was supported by JSPS KAKENHI Grant Number 25-9627.

The authors thank Mr. R. Kaida from Department of Mathematical Engineering and Information Physics, The University of Tokyo for his significant contribution.

REFERENCES

- [1] M. Fujiwara, K. Nakatsuma, M. Takahashi, and H. Shinoda, "Remote Measurement of Surface Compliance Distribution Using Ultrasound Radiation Pressure", *Proc. IEEE World Haptics Conference 2011*, Istanbul, Turkey, pp. 43-47, 2011.
- [2] T. Hoshi, T. Iwamoto, and H. Shinoda, "Non-contact Tactile Sensation Synthesized by Ultrasound Transducers," *IEEE Transaction on Haptics*, vol. 3, no. 3, pp. 256-260, Jan. 2010.
- [3] T. Hasegawa, T. Kido, T. Iizuka, C. Matsuoka, "A general theory of Rayleigh and Langevin radiation pressures," *Journal of Acoustical Society of Japan*, vol. 21, no. 3, pp. 145-152, 2000.
- [4] M. Fujiwara and H. Shinoda, "Remote Measurement Method of Surface Compliance Distribution for a Curved Surface Object," *Proc. SICE Annual Conference 2012*, pp.1-5, August, 2012.
- [5] B. D. Lawrence and J. A. Simmons, "Measurements of atmospheric attenuation at ultrasonic frequencies and the significance for echolocation by bats," *Journal of the Acoustical Society of America*, vol. 71, no. 3, pp. 585-590, 1987.